# Reliability of built-up cold-formed beams subjected to bending

Marcelo B. Pereira[1] , André L. R. Brandão[2], Marcílio S. R. Freitas[1]

[1]*Civil Engineering Program, Federal University of Ouro Preto*
*Ouro Preto, 35.400-000, Minas Gerais, Brazil*
*marcelo.borges@aluno.ufop.edu.br, marcilio@ufop.edu.br*
[2]*Institute of Integrated Engineering, Federal University of Itajubá*
*Itabira, 37.500-903, Minas Gerais, Brazil*
*andreriqueira@unifei.edu.br*

**Abstract.** The use of cold-formed steel (CFS) members in structural engineering is increasing due to their structural and environmental advantages, such as low weight, ease and speed of construction, greater manufacturing flexibility and recyclability. Despite the common use of CFS built-up sections subjected to bending, the structural design of these sections needs further investigation. This work aims to critically review research on the structural behavior and design methodology of these elements, as well as evaluate the reliability indices of built-up sections subjected to bending using the FOSM, FORM and Monte Carlo Simulation methods. The safety of built-up sections designed using the Direct Strength Method was verified. A statistical analysis of the professional factor was developed from an experimental database and the structural safety of the bars was verified using first-order reliability methods to assess the level of safety for different combinations of actions. In general, the average values of the professional factor show low dispersion, reflected in the low coefficients of variation. The reliability indices for the LRFD showed good results, and no reliability index for the combination referring to the LSD and NBR methods reached its target.

**Keywords:** Built-up beams; DSM; FORM; Reliability; Cold-formed steel.

## 1 Introduction

NBR 14762 [1] defines cold-formed steel (CFS) as elements made up of steel sheets bent at room temperature in a continuous or discontinuous bending process. These profiles have been gaining ground in the market due to their economy, speed and sustainability and, according to Yu [2], can be efficiently used in warehouses, mezzanines, industrial storage systems and Light Steel Frame systems. According to Javaroni [3] and Freitas *et al*. [4], the Direct Strength Method (DSM) can be used to calculate the strength of cold-formed profiles, which uses elastic local buckling stresses for the profile as a whole and geometric properties of the gross section to predict local and distortional buckling modes.

Wang and Young [5] state that cold-formed steel sections are often produced in asymmetrical or monosymmetrical open sections, offering flexibility and ease of manufacture. However, the torsional rigidity of these open sections is relatively low. To overcome this problem, CFS built-up sections can be configured into doubly symmetrical sections. Figure 1 shows some examples of built-up sections.

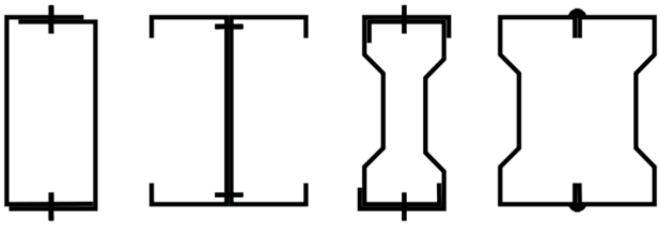

Figure 1 - Example of built-up sections (adapted from Rasmussen *et al.*[6])

Built-up bars are widely used in construction today, but there are few specific guidelines in design standards for their design. Generally, the sum of the capacities of the individual profiles is adopted, which results in an excessively conservative approach, Andrade *et al*. [7]. According to Georgieva, Schueremans and Vandewalle [8], engineers often adopt conservative assumptions when designing built-up members in CFS, based on their experience and judgment. It is therefore essential to study variations of the direct strength method that take into account crucial aspects of built-up member behavior, such as sensitivity to imperfections, different buckling modes and uncertainties related to material properties, the manufacturing process and the analysis method, for example.

The aim of this work is to critically review research into the structural behavior and design methodology of these elements. It also evaluates the reliability indices ($\beta$) of built-up sections subjected to bending, using the First Order Second Moment (FOSM), First Order Reliability Method (FORM) and Monte Carlo Simulation (MCS) reliability methods, verifying the safety of these bars designed using the Direct Strength Method.

## 2 Theoretical nominal strength

The available flexural strength ($M_n$), calculated by the DSM, shall be the smallest value between: the nominal flexural strength for global buckling ($M_{ne}$), the nominal flexural strength for local buckling ($M_{nl}$) and the nominal flexural strength for distortional buckling($M_{nd}$), Toledo *et al* [9]. Equations 1 to 5 show the functions set out in AISI S100 [10] for calculating these strength moments.

### 2.1 Lateral-torsional buckling (global)

$$M_{ne} = \begin{cases} M_{cre}, \quad M_{cre} < 0.56M_y \\ \frac{10}{9}M_y\left(1 - \frac{10M_y}{36M_{cre}}\right), \quad 2.78M_y \geq M_{cre} \geq 0.56M_y \\ M_y, \quad M_{cre} < 2.78M_y \end{cases} \tag{1}$$

where $M_{cre}$ is the critical elastic lateral-torsional bucking moment and $M_y$ is the member yield moment.

### 2.2 Local buckling

$$\lambda_l = \sqrt{\frac{M_{ne}}{M_{crl}}} \tag{2}$$

$$M_{nl} = \begin{cases} M_{ne}, \quad \lambda_l \leq 0.776 \\ \left[1 - 0.15\left(\frac{M_{crl}}{M_{ne}}\right)^{0.4}\right]\left(\frac{M_{crl}}{M_{ne}}\right)^{0.4} M_{ne}, \quad \lambda_l > 0.776 \end{cases} \tag{3}$$

where $M_{crl}$ is the critical elastic local bucking moment and $\lambda_l$ is the slenderness index for local buckling.

### 2.3 Distortional buckling

$$\lambda_d = \sqrt{\frac{M_y}{M_{crd}}} \tag{4}$$

$$M_{nd} = \begin{cases} M_y, \quad \lambda_d \leq 0.673 \\ \left[1 - 0.22\left(\frac{M_{crd}}{M_y}\right)^{0.5}\right]\left(\frac{M_{crd}}{M_y}\right)^{0.5} M_y, \quad \lambda_d > 0.673 \end{cases} \tag{5}$$

where $M_{crd}$ is the critical elastic distortional bucking moment and $\lambda_d$ is the slenderness index relative to distortional buckling.

# 3 Structural reliability

According to Haldar and Mahadevan [11], engineering projects usually operate on a fine line, seeking to increase the safety of the structure while at the same time making it viable and economical. These projects can be complex and face a number of significant uncertainties, and some of these uncertainties are unavoidable and must be considered as early as the design phase. Design uncertainties range from the natural randomness of actions to human errors in the design, execution and operation of the structure. Nowak and Collins [12] present three categories of sources or causes of uncertainties in the strength of a structural component: uncertainties in the properties of the material, in the manufacturing process and in the method of analysis. Each of these factors can be considered a random variable, just like the strength itself. The final strength is then determined by multiplying the nominal strength by these three factors.

The most common design method today, which incorporates probabilistic concepts into the design of structures, is the Limit State Method. This method assigns weighting coefficients to both the actions and the strength of structural elements, taking into account their variability. The reliability methods used to calibrate these coefficients use the $\beta$ as a safety parameter or the probability of failure [12]. Three of the most common reliability methods for finding $\beta$ are presented below.

## 3.1 FOSM method

According to Hsiao [13], the FOSM (First Order Second Moment) method uses the averages of the strength $\mathrm{R_m}$ and request $\mathrm{Q_m}$ and their respective standard deviations $\sigma_R$ e $\sigma_Q$. Although the method was initially developed for normal distributions, it is assumed that Q and R follow the lognormal probability distribution. Equation 8 presents a mathematical reorganization of the formula for calculating the reliability index, which allows for the consideration of lognormal distributions, where $V_R$ and $V_Q$ are the coefficients of variation of R and Q, for R and Q independent of each other. The limitations of the FOSM method, however, are associated with the fact that it only considers the normal or lognormal distribution for the variables and the statistical independence between them.

$$\beta = \frac{ln\frac{R_m}{Q_m}}{\sqrt{V_R^2+V_Q^2}} \tag{8}$$

## 3.2 FORM method

The FORM (First Order Reliability Method) method performs Taylor series expansion around a point called the design point and transforms random variables of known probability distribution into statistically independent standard normal variables, Low and Tang [14]. The random variables are transformed to the reduced space and the failure surface is approximated by a linear surface at the point closest to the origin, which is the design point. The value of $\beta$ is then given by the distance from the origin to the design point.

## 3.3 Monte Carlo simulation

MCS consists of sampling basic variables according to their probabilistic characteristics and then applying them to a failure function [15]. It is a repetition process that generates deterministic solutions to a given problem; each solution corresponds to a set of deterministic values of a set of underlying random variables [16]. The probability of failure is the ratio between the number of times a simulation has failed, i.e. the limit state function has been less than or equal to 0, and the number of simulations generated. The accuracy of this method depends on the number of simulations carried out.

# 4 Methodology

The database used contains 35 built-up test specimens, divided into 18 open sections and 17 closed sections, Wang and Young [5]. The open sections are formed by joining two stiffened U-sections, resulting in an I-section, while the closed sections are created by connecting two simple U-sections, forming a box section. Figure 2 shows the sections geometry used by the author. To calculate the theoretical resisting moments was used the DSM and the software CUFSM v5.01 [17] was used to analyze the elastic instability of the sections, identifying the critical local and distortional buckling moments.

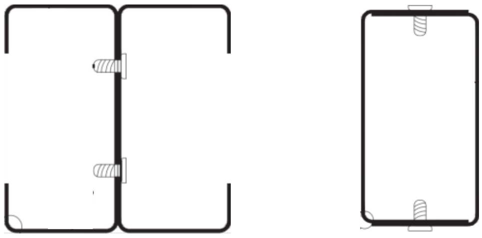

a) Open section b) Closed section

Figure 2: Sections geometry used by Wang and Young

The Professional Factor (P) was treated as a random variable and analyzed in three groups: open sections, closed sections and all built-up sections. Using the software MINITAB 19 [18], the most appropriate probability distribution for the data was selected using the Anderson-Darling test, considering six probability density functions (Normal, Lognormal, Gumbel maximum and minimum, Weibull and Gamma). Using Microsoft Excel [19], the FOSM, FORM and MCS methods were implemented to calculate the reliability indices β and the probability of failure $P_f$ . The FORM method converged in five iteractions, with a tolerance of $3.10^{-5}$, MCS performed 200,000 simulations and its input data is described in Tables 1 and 2.

Table 1: Input data for the load combinations

| Standard | $\phi$ | $\gamma_D$ | $\gamma_L$ | $\rho$ | $\beta_0$ |
|---|---|---|---|---|---|
| LRFD | 0.90 | 1.20 | 1.60 | 5.0 | 2.5 |
| LSD | 0.90 | 1.25 | 1.50 | 3.0 | 3.0 |
| NBR | 0.91 | 1.25 | 1.50 | 3.0 | 2.5 |
| NBR | 0.91 | 1.25 | 1.50 | 5.0 | 2.5 |

Table 2. Statistical data for the variables

| Variable | M | F | D | L |
|---|---|---|---|---|
| $\mu$ | 1.10 | 1.00 | 1.05 | 1.00 |
| $\sigma$ | 0.11 | 0.05 | 0.10 | 0.25 |
| COV | 0.10 | 0.05 | 0.10 | 0.25 |
| PDF | Lognormal | Lognormal | Normal | Gumbel maximum |

Table 1 shows the resistance factor $\phi$, load factor $\gamma$, the ratio $L_n/D_n = \rho$, with $L_n$ and $D_n$ being, respectively, the nominal values of live and dead loads, as well as the target reliability indices $\beta_0$ for each load combination from AISI S100 [10] specification for LRFD and LSD and the NBR 14762 [1] code. Table 2 presents the mean ($\mu$); standard deviation ($\sigma$); coefficient of variation (COV) and probability density function (PDF) to the uncertainties of the material M, called the "material factor", and geometric property variability F, called the "fabrication factor", both prescribed in the NBR for the situation studied. For the loads, D and L represent the dead and live load variables, respectively, as proposed by Galambos *et al*. [20].

Equation 9 shows the limit state function provided by the specification, where $R_n$ represent the nominal strength. Assuming that, at the limit, the resistance is equal to the calculation load in equation 9, the nominal actions can be rewritten as a function of the nominal resistance and the defined $\rho$ ratio, according to Equations 10 and 11. Equation 12 shows the proposed failure function based on the usual limit state safety conditions and considering only dead and live loads variable with their deterministic coefficient related to the intensity of the load (c) and leaving the strength as a function of the coefficients P, M and F.

$$\phi R_n \geq \gamma_D D_n + \gamma_L L_n \quad (9)$$

$$D_n = \frac{\phi R_n}{(\gamma_D + \rho \gamma_L)} \quad (10)$$

$$L_n = \frac{\phi R_n}{\left(\frac{\gamma_D}{\rho} + \gamma_L\right)} \quad (11)$$

$$G(.) = R_n \mathrm{MFP} - \mathrm{c(D + L)} \quad (12)$$

# 5 Results

## 5.1 Comparison between nominal and experimental moments

Considering the three possible failure modes, none of the built-up sections analyzed failed due to global buckling and this can be explained by the greater stiffness attributed to the built-up sections in addition to the modest buckling length of the test specimens. Figure 3 shows the values of the experimental ultimate moments, in which the vertical axis is normalized to the yield moment My, of the test specimens compared with the nominal resisting moments related to local and distortional buckling, for open and closed sections, referring to the work by Wang and Young [5].

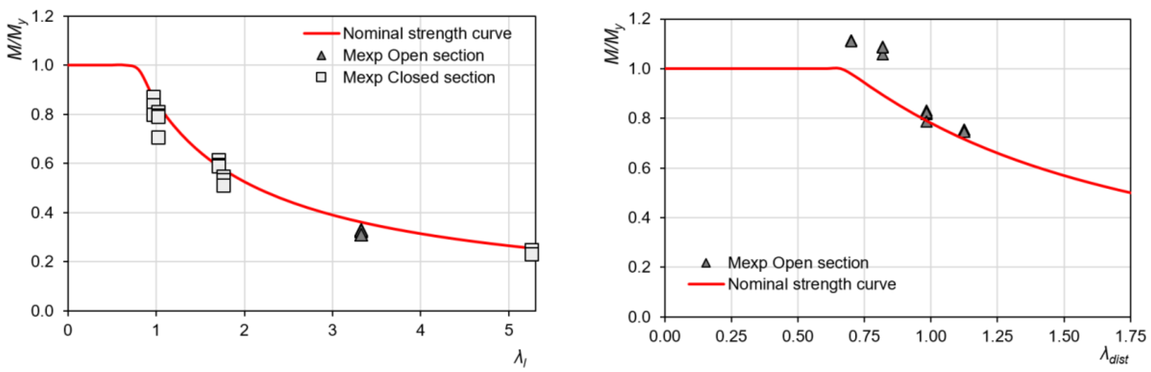


a) Local buckling b) Distortional buckling

Figure 3: Comparison of normalized experimental results of the test specimens with the nominal values

Among the test specimens analyzed, all the closed-section profiles failed due to local buckling. This behavior is justified by the flanges connections, which hinder the distortional mode of buckling. For both open and closed sections, the normalized experimental ultimate moments are close to the nominal strength curve, most of them below it. However, this trend may vary as the database for this work be expanded. The distortional buckling failure mode was the least common, being observed only in open sections, as expected. Just like in the local buckling mode, the normalized experimental results of the test specimens that failed due to distortional buckling exhibited a graphical behaviour pattern similar to that of the nominal strength curve, although slightly more distant than in the case of local buckling failure. Looking at the plots, it can be seen that the equations for the distortion mode are slightly conservative. It can also be seen that the equations for the local mode are slightly unconservative, as the theoretical values overestimate the experimental results. This observation, although marginal, suggests the opportunity to investigate variations in the DSM that may better align with the normalized experimental values.

## 5.2 Professional factor

Table 3 shows a statistical summary, with quantity (Nr); mean; standard deviation and coefficient of variation of the P values found and the PDF adjusted for each grouping in the database. In general, the average P values are close to 1.0 and have low coefficient of variation values, which indicates low dispersion in the results. This may contribute to lower probability of failure values, depending on the PDF, and indicates that conventional DSM is a good fit for this database.

Table 3: Statistics of the professional factor of the data groups

| Data Group | Nr | $\mu$ | $\sigma$ | COV | PDF adjusted |
|---|---|---|---|---|---|
| Open sections | 17 | 1.052 | 0.107 | 0.102 | Normal |
| Closed sections | 18 | 0.958 | 0.051 | 0.053 | Weibull |
| All sections | 35 | 1.006 | 0.096 | 0.095 | Gumbel maximum |

### 5.3 Reliability analysis

Figure 4 shows the graph with the β values calculated by the FOSM, FORM and MCS reliability methods for open and closed sections. The bars with the letter "O" in their nomenclature refer to open sections and those with "C" refer to closed sections. Each group of members represents a combination used to calibrate the standards.

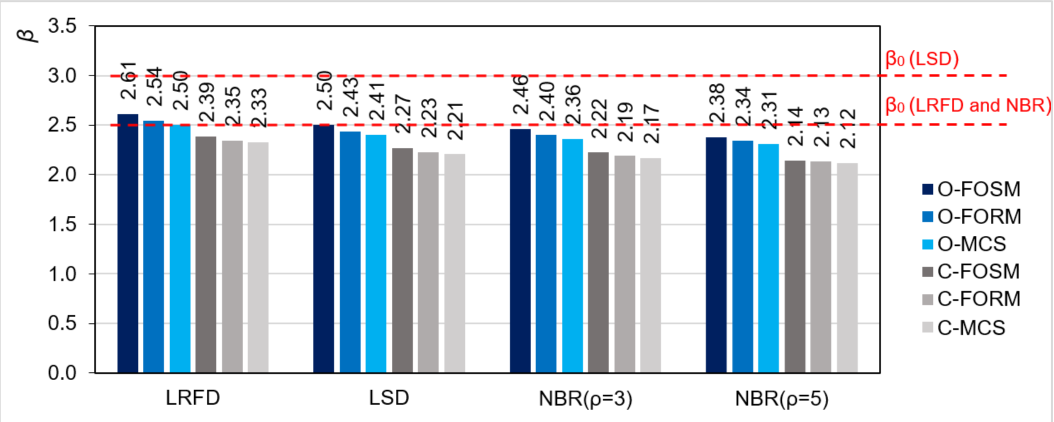


Figure 4: Reliability indices using the FOSM, FORM and MCS methods for open and closed sections for the four combinations studied.

As expected, the reliability indices obtained by the FORM method were close to those obtained via MCS, since they are more precise methodologies compared to FOSM. The group of open sections generally showed better results than the group of closed sections. The open section group, considering the LRFD combinations, was the only one to achieve results equal to or greater than its target reliability index ($\beta_0$). No LSD combination reliability index reached its $\beta_0$, being closer to the target β of 2.5. On the other hand, NBR results are closest although it didn't reach its target either. Of the two NBR loading ratios, the one with ρ=3 showed the highest $\beta$ values.

## 6 Conclusions

In summary, analysis of the statistical results reveals that the average P values were close to 1.0 and showed low dispersion, reflected in the low coefficients of variation. In the experimental data, all the closed sections failed by local buckling, while the open sections failed predominantly by distortional buckling. Reliability, as measured by the $\beta$ indices, varied according to the method and specifications, with the FORM and MCS methods showing similar and more accurate results compared to FOSM. The open sections showed greater reliability than the closed ones, especially in the LRFD combinations, while the LSD and NBR combinations did not reach their target reliability indices, although the NBR came closest. These findings indicate that, although DSM provides a good fit to the database studied, there is potential to adjust the model to align even better with the experimental values, improving the accuracy and reliability of the predictions.

**Acknowledgements.** This study was financed in part by the Coordenação de Aperfeiçoamento de Pessoal de Nível Superior - Brasil (CAPES) - Finance Code 001. The authors are grateful to the Federal University of Ouro Preto (UFOP).

**Authorship statement.** The authors hereby confirm that they are the sole liable persons responsible for the authorship of this work, and that all material that has been herein included as part of the present paper is either the property (and authorship) of the authors, or has the permission of the owners to be included here.

## References

[1] ABNT. NBR 14762: Dimensionamento de estruturas de aço constituídas por perfis formados a frio. Rio de Janeiro: Associação Brasileira de Normas Técnicas, 2010. https://doi.org/01.080.10; 13.220.99.
[2] C. Yu, "Recent Trends in Cold-Formed Steel Construction". Woodhead Publishing. *Series in Civil and Structural Engineering*, n. 65, 2016.
[3] C. E. Javaroni, "Estruturas de Aço: Dimensionamento de Perfis Formados a Frio". Rio de Janeiro: *Elsevier*, 2015.
[4] M. S. R. Freitas, A. L. R. Brandão, A. M. S. Freitas, "Resistance factor calibration for cold-formed steel compression members". *REM. Revista Escola de Minas*, v. 66, pp. 233-238, 2013.
[5] L. Wang and B. Young, "Behavior and design of cold-formed steel built-up section beams with different screw arrangements". *Thin-Walled Structures*, vol.131, pp. 165-32, 2018.
[6] K.J.R. Rasmussen, M. Khezri, B.W. Schafer, H. Zhang, "The mechanics of built-up cold-formed steel members". *Thin-Walled Structures*, vol. 154, pp. 0263-8231, 2020.
[7] C. P. Andrade, M. S. R. Freitas and A. L. R. Brandão. "Reliability of built-up cold-formed steel columns designed by the direct strength method". In: XLIII IberianLatin American Congress on Computational Methods in Engineering, pp. 1-7, 2022.
[8] I. B. Georgieva, L. P. L. Schueremans and L. Vandewalle, "Innovative cross-section shapes for built-up CFS columns. Experimental investigation". *21st International Speciality Conference on Cold-formed Steel Structures*, 2012.
[9] F. F. A. Toledo, M. S. R. Freitas and A. L. R. Brandão, "Reliability assessment of cold-formed steel beams by the FORM method". *REM – International Engineering Journal*, v. 74, pp. 183-188, 2021.
[10] AISI. AISI S100: North American Specification for the Design of Cold-Formed Steel Structural Members. Washington, DC: AISI, 2016.
[11] A. Haldar and S. Mahadevan, "Probability, Reliability and Statistical Methods in Engineering Design". New York, NY: *John Wiley & Sons*, 2000.
[12] A. S. Nowak and K . R. Collins, "Reliability of Structures". *USA: McGraw-Hill*, 2000. vol. 259, . https://doi.org/10.1016/j.nimb.2007.01.180.
[13] L.E. Hsiao. Reliability Based Criteria for Cold-Formed Steel Members. PhD thesis, University of Missouri-Rolla, 1989.
[14] B. K. Low and W. H. Tang, "Reliability Analysis Using Object-Oriented Constrained Optimization". *Struct. Saf*, vol. 26, n. 1, pp. 69-89, 2004.
[15] B. M. Ayyub and R. H. McCuen, "Probability, Statistics, and Reliability for Engineers". *Boca Raton: CRC Press*, vol. 93, 2011 . https://doi.org/10.2307/2669892.
[16] A. H. S. Ang and W. H. Tang, "Probability Concepts in Engineering Planning and Design: Vol. II-Decision, Risk and Reliability". *USA: John Wiley & Sons*, vol. 2, 1990 . https://doi.org/10.2307/2987875.
[17] CUFSM: conventional and constrained finite strip methods. Orlando, FL, 2018.
[18] MINITAB LLC. MINITAB 19. 2019.
[19] MICROSOFT CORPORATION. Microsoft Excel 2016. Redmond, WA, 2016.
[20] T. V. Galambos, B. Ellingwod, J. G. Macgregor and C. A. Cornell, "Probability Based Load Criteria: Assessment of Current Design Practice". *Journal of the Structural Division*, pp. 1409-1426, 1982.